The bilingual structural connectome: Dual-language experiential factors modulate distinct cerebral networks

Davide Fedeli [a], Nicola Del Maschio [a], Simone Sulpizio [b,c], Jason Rothman [d,e], Jubin Abutalebi [a,d,*]

[a] Centre for Neurolinguistics and Psycholinguistics, Faculty of Psychology, Vita-Salute San Raffaele University, Italy
[b] Department of Psychology, University of Milano-Bicocca, Italy
[c] Milan Center for Neuroscience (NeuroMI), University of Milano-Bicocca, Italy
[d] The Arctic University of Norway, Tromsø, Norway
[e] Universidad Antonio de Nebrija, Madrid, Spain

ARTICLE INFO

ABSTRACT

Bilingualism is a natural laboratory for studying whether the brain's structural connectome is influenced by different aspects of language experience. However, evidence on how distinct components of bilingual experience may contribute to structural brain adaptations is mixed. The lack of consistency, however, may depend, at least in part, on methodological choices in data acquisition and processing. Herein, we adopted the Network Neuroscience framework to investigate how individual differences in second language (L2) exposure, proficiency, and age of acquisition (AoA) – measured as continuous between-subject variables – relate to whole-brain structural organization. We observed that L2 exposure modulated the connectivity of two networks of regions subserving language comprehension and production. L2 proficiency was associated with enhanced connectivity within a rostro-caudal network, which supports language selection and word learning. Moreover, L2 AoA and exposure affected inter-hemispheric communication between control-related regions. These findings expand mechanistic knowledge about particular environmental factors associated with specific variation in brain structure.

1. Introduction

The brain's white matter (WM) is composed of myelin-coated bundles of axons that enable efficient information transfer between neighbouring and distant regions of the brain. WM is highly prone to learning-dependent structural changes, even beyond temporal periods of higher plasticity such as early development (Sampaio-Baptista & Johansen-Berg, 2017). In recent years, there has been increased interest in examining WM adaptation in response to the learning and regulation of a dual language system, a prime example of complex skill acquisition (see, for review, Pliatsikas, 2019). Whereas input leads to activation of a single language system in monolinguals, in individuals who speak (or sign) in two languages both systems are simultaneously activated in production and comprehension automatically (e.g., Hoshino & Thierry, 2011; Kroll, Sumutka, & Schwartz, 2005). The co-activation of both languages is thought to give rise to cross-language competition that must

be resolved for communication to proceed (e.g., Hermans, Bongaerts, de Bot, & Schreuder, 1998; Marian & Spivey, 2003; Abutalebi & Green, 2007). The context-dependent use of a target language for communicative purposes, in the face of co-activation and potential competition between languages, has been associated with heightened recruitment of top-down control processes for bilinguals (Green & Abutalebi, 2013; Green, 1998; Kroll, Bobb, Misra, & Guo, 2008). This is especially true for late second language (L2) learners and poorly proficient or less exposed bilingual users, who seem to experience additional cognitive effort than highly immersed or proficient bilinguals when coordinating between languages (Del Maschio & Abutalebi, 2019; Sulpizio, Del Maschio, Del Mauro, Fedeli, & Abutalebi, 2020).

At the neural level, in analogy with the principle that skill-based training shapes training-related neural circuits, bilingualism has been shown to drive structural changes in regions and networks engaged by bilingual language processing (that is, perhaps among other functions,

language learning, processing and control). Of note, previous neuroimaging studies investigating the structural effects of bilingualism in adults (measured as differences between bilingual and monolingual groups, or occasionally in training studies) have adopted Tract-Based Spatial Statistics (TBSS) (Cummine & Boliek, 2013). TBSS enables whole-brain mapping of diffusion parameters such as Fractional Anisotropy (FA), a scalar measure which quantifies the degree of water diffusivity anisotropy and is associated with axonal diameter, fiber density, and myelination. Both longitudinal and cross-sectional studies have frequently found higher FA values in the bilateral Superior Longitudinal Fasciculus (SLF), the Inferior Frontal Occipital Fasciculus (IFOF), and portions of the Corpus Callosum (CC) as a consequence of bilingual experience (e.g., Del Maschio et al., 2019c; Hosoda, Tanaka, Nariai, Honda, & Hanakawa, 2013; Kuhl et al., 2016; Luk, Bialystok, Craik, & Grady, 2011). These results may fit with dual-stream models of spoken language processing in which dorsal and ventral pathways support distinct linguistic functions (Hickok & Poeppel, 2004; Saur et al., 2008), and with models of efficient dual-language control underpinned by a bilaterally distributed cortico-subcortical network associated with executive control processes (Abutalebi & Green, 2016; Calabria, Costa, Green, & Abutalebi, 2018). However, not all studies replicate these findings. Instead, some have shown decreased FA values in bilingual individuals in SLF, IFOF, and CC (Elmer, Hänggi, Meyer, & Jäncke, 2011; Gold, Johnson, & Powell, 2013) whereas others have reported significant WM plasticity effects ascribable to bilingualism, but only when using different microstructural indices, such as Axial, Radial, and Mean Diffusivity (Cummine & Boliek, 2013; Kuhl et al., 2016; Singh et al., 2018).

The above-referenced incongruencies may be partially related to intrinsic aspects of TBSS. Despite its popularity, TBSS is indeed significantly limited in its anatomical accuracy for reconstructing WM pathways (Bach et al., 2014; Hämäläinen, Sairanen, Leminen, & Lehtonen, 2017), and permits only a glimpse into local voxel-based effects. Thus, it is under-/uninformative of larger-scale interregional communication. Moreover, WM microstructural measures have been typically estimated from diffusion data modeled with the diffusion tensor, a technique named Diffusion Tensor Imaging (DTI). All previous diffusion MRI studies on bilingualism except one (Rahmani, Sobhani, & Aarabi, 2017) had adopted DTI as a diffusion modeling technique. The methodological literature agrees there is a need to move beyond DTI, which suffers from intrinsic limitations and is unable to provide a reliable reconstruction of the crossing fibers that are contained in more than 90% of WM voxels (Farquharson et al., 2013; Jeurissen, Leemans, Tournier, Jones, & Sijbers, 2013; Jones, Knösche, & Turner, 2013). These considerations suggest that the current literature on WM changes associated with bilingual experience still suffers from a set of methodological constraints that prevent one from getting a clear understanding of the phenomenon of interest.

Over the last ten years, Network Neuroscience has emerged as an experimental framework to investigate brain structural and functional organization (Bullmore & Sporns, 2009; Rubinov & Sporns, 2010). This approach, also known as Connectomics, conceptualizes the brain as a complex network of nodes (brain regions) and edges (connections), and uses the tools and methods of network science and graph theory to define the principles of its organization. Moreover, Network Neuroscience allows one to quantify whether and to what extent internal and external factors (e.g., pathology, treatment, training) influence the topological properties of the brain connectome as a complex system (i.e., the matrix of all possible pairwise connections between brain regions) (see Fornito, Zalesky, & Bullmore, 2016). Recently, Li and Grant (2016) have highlighted the benefits of implementing this approach in bilingualism research, especially by adopting network efficiency metrics for defining the dynamics of structural and functional reorganization in L2 learners. According to the authors, by revealing changes in the relationships among multiple brain regions, the connectivity approach represents a promising tool to uncover crucial effects of bilingual

experience that previous studies focused on single regions/activations could not detect. In the present study, we capitalize on Network Neuroscience with the aim to investigate how distinct components of bilingual experience – i.e., L2 Age of Acquisition (AoA), L2 Proficiency, and L2 Exposure – modulate brain structural connectivity. As underscored recently by Surrain and Luk (2017) and Leivada, Westergaard, Duñabeitia, and Rothman (2021), among others, the surge in research comparing bilinguals and monolinguals as binary groups, along with the use of different criteria for determining who is bilingual, likely contributes to diverse and often conflicting data. Grouping heterogeneous linguistic profiles under a dichotomous condition may obscure, if not wash out, important, yet distinct facets of the bilingual experience, which is dynamic and complex at the individual level. Moreover, focusing on a single attribute of bilingual experience, or simply testing the individual effects of different dimensions, prevents obstacles for detecting whether (and to what extent) these dimensions interact with each other in shaping experience-dependent structural plasticity. On these grounds, and in line with recent trends in the neuroscience of bilingualism (e.g., Li, Legault, & Litcofsky, 2014; Deluca, Rothman, & Pliatsikas, 2019; DeLuca, Rothman, Bialystok, & Pliatsikas, 2019, DeLuca, Rothman, Bialystok, & Pliatsikas, 2020; Kousaie, Chai, Sander, & Klein, 2017; Sulpizio, Del Maschio, Del Mauro et al., 2020), we used whole-brain probabilistic WM tractography to examine bilingual experience as a continuous and multi-componential construct in a sample of native Italian speakers who spoke English as an L2 (N = 77). To reach this aim, we adopted state-of-the-art diffusion modelling and processing techniques (e.g., Constrained Spherical Deconvolution and Anatomically Constrained Tractography, Multi-Shell diffusion MRI acquisition) to overcome the methodological limitations of previous research.

We expect that the Network Neuroscience framework will reveal a set of distinct and overlapping language/executive regions that reflect the specific contribution of L2 AoA, Proficiency, and Exposure in driving brain structural plasticity and organization. We rely on graph theory as a tool to describe the topological properties of these networks, such as identifying the nodes with the highest number of connections, those that act as a central communication hub, and those grouped in modular subsystems. Hence, graph theoretical measures will allow us not only to deconstruct the bilingual structural connectome in its fundamental experience-related components, but also to provide a comprehensive description of how L2 experience changes the relationship between the regions that are part of these networks. For example, measures of centrality (e.g. node degree, betweenness centrality) permits a description of whether one brain region plays a peripheral role in a network related to L2 proficiency despite its central importance in a network modulated by L2 exposure. Moreover, detecting clusters of connected regions within one network (e.g. by modularity measures) reveals areas of community specialization that may enrich functional models of L2 information processing and bilingualism-induced brain plasticity. Finally, and in line with recent structural and functional connectivity studies on bilingualism (García-Pentón, Fernández, Iturria-Medina, Gillon-Dowens, & Carreiras, 2014; Sulpizio, Del Maschio, Del Mauro et al., 2020), we use graph theory to investigate the degree of interconnectedness (e.g. local and global efficiency) of relevant networks. This is expected to provide insightful information on the broad impact of bilingual experience in reshaping the connectivity at the whole-brain level.

2. Materials and methods

2.1. Participants

Seventy-seven (n = 77) young adult participants took part in the study (46F; mean age = 25.27, SD = 4; mean years of formal education = 17.1, SD = 1.86). All participants were right-handed, as assessed by the Edinburgh Handedness Inventory scale (Oldfield, 1971), had normal or corrected-to-normal vision, and no history of psychiatric or neurological disorders. Participants' Socio-Economic Status (SES) was

measured with The MacArthur Scale of Subjective Social Status (https://macses.ucsf.edu/research/psychosocial/subjective.php#measurement). All participants were native Italian speakers who spoke English as a second language (L2). Measures quantifying L2 Age of Acquisition (AoA), L2 Proficiency, L2 daily Exposure, and Language Switching habits were collected for each participant. L2 AoA was assessed by means of a self-report questionnaire. L2 Proficiency was tested with two objective measures: 1) the online Cambridge Test for adult learners (http://www.cambridgeenglish.org/test-your-english/general-english/), which consist in 25 items that assess grammatical and conversational knowledge (see Sulpizio et al., 2019) and 2) an L1-to-L2 Translation Test, which consist of 30 high-frequency, 30 medium-frequency, and 30 low-frequency words (Van Heuven, Mandera, Keuleers, & Brysbaert, 2014). L2 Exposure was computed using a self-report questionnaire in which each participant was asked to report how many hours per day s/he used the L2 in different contexts (i.e., family, friends and/or classmates, partner, study and/or job, reading and writing, media, other activities). Patterns of language switching behavior were estimated using the Bilingual Switching Questionnaire (BSWQ; Rodriguez-Fornells, Kramer, Lorenzo-Seva, Festman, & Münte, 2012). Participants were asked to evaluate their language switching habits using a five-point scale (from 1-never to 5-always). The questionnaire can be decomposed into four indices (3 items per index) corresponding to different aspects of switching behavior (L1 switching tendencies, L1s = the tendency to switch to L1; L2 switching tendencies, L2s = the tendency to switch to L2; contextual switch, CS = the frequency of switches in particular situations or environments; unintended switch, US = the lack of awareness of language switches). Fluid and verbal intelligence were assessed, respectively, with the Raven's Standard Progressive Matrices for adults (the intelligence quotient was estimated based on normative data for the Italian population; Basso, Capitani, & Laiacona, 1987), and the Test di Intelligenza Breve (TIB; Colombo, Sartori, & Brivio, 2002), the Italian equivalent of the National Adult Reading Test (NART; Nelson, 1982). The demographic, cognitive, and linguistic characteristics of the sample are reported in Table 1.

The present study was conducted with ethical approval from the Human Research Ethics Committee of the Vita-Salute San Raffaele University (Milan, Italy). Written informed consent was obtained from all participants.

2.2. MRI acquisition

MRI acquisition was performed at the Centro di Eccellenza Risonanza Magnetica ad Alto Campo (C.E.R.M.A.C.), Vita-Salute San Raffaele University/San Raffaele Hospital, Milan (Italy) by means of a 3-T Philips Ingenia CX MR scanner (Philips Medical Systems, Best, Netherlands) with a 32 channels SENSE head coil. A high-resolution Magnetization Prepared Rapid Gradient Echo (MPRAGE) T1-weighted anatomical image was acquired for each participant with the following parameters: repetition time (TR) = 9.9 ms, echo time (TE) = 4.9 ms, flip angle = 8°, FOV = 260 mm, matrix size = 256 × 256, number of axial slices = 243, slice thickness = 1.4 mm, voxel size = 0.7 × 0.7 × 0.7 mm 3, Phase Encoding direction (PE) = A/P, SENSE factor = 2, with whole brain coverage.

Diffusion weighted images (DWI) were acquired with a multi-shell sequence (applied b values = 700, 1000, 2855 s/mm2 , in 6, 30, and 60 gradient directions respectively, with 10 b0 images distributed within the sequence) with the following parameters: 106 diffusion-encoding gradient directions, TR = 5900 ms, TE = 78 ms, flip angle = 90°, FOV = 240 mm, matrix size = 128 × 128, number of axial slices = 56, slice thickness = 2.3, voxel size = 1.875 × 1.875 × 2.3 mm, PE = A/P, SENSE factor = 2, with whole brain coverage. Additionally, four b = 0 images were collected with reversed phase-encode blips (i.e., volumes with distortions going in opposite direction) for distortion correction purposes.

2.3. Diffusion MRI Preprocessing

Diffusion MRI preprocessing was performed with the open-source software MRtrix3 (Tournier et al., 2019), which implements several different options of voxel-level modelling, including Multi-Shell Multi-Tissue Constrained Spherical Deconvolution (MSMT CSD, Jeurissen, Tournier, Dhollander, Connelly, & Sijbers, 2014). For every participant, the following pipeline was adopted for data cleansing and voxel-level modelling: i) visual inspection for major artifacts; ii) data denoising to enhance signal-to-noise ratio (SNR) (Veraart et al., 2016); iii) Gibbs ringing artefacts removal (unringing) (Kellner, Dhital, Kiselev, & Reisert, 2016); iv) motion and distortion correction (Andersson & Sotiropoulos, 2016; Andersson, Graham, Zsoldos, & Sotiropoulos, 2016), with Topup and Eddy tools implemented from FSL (Smith et al., 2004); v) estimation of Fiber Orientation Distribution (FOD) (Tournier et al., 2019) with the "Dhollander" algorithm, which adopts MSMT CSD to take advantage of the multiple b-values to overcome potential biases occurring in voxels with partial volumes (e.g., voxels containing both grey and white matter), and permits an accurate estimation of the orientation of all fibers crossing each voxel of the brain (Dhollander, Raffelt, & Connelly, 2016, 2019) and vi) intensity normalization to correct for effects of residual intensity inhomogeneities. Diffusion MRI preprocessing, along with subsequent analyses steps, are illustrated in Fig. 1.

2.4. Anatomically Constrained Tractography

After data preprocessing, Anatomically Constrained Tractography (ACT) was performed (Smith, Tournier, Calamante, & Connelly, 2012). ACT uses anatomical priors from high-resolution T1-weighted images as a reference to reconstruct only biologically plausible white matter fibres trajectories, thus improving the overall accuracy of streamline generation (e.g., ACT allows to reject unrealistic streamlines that end in Cerebrospinal Fluid). This method is particularly suited for connectome construction and subsequent network analyses where nodes are generated from grey matter parcellations, since streamlines terminate only in valid areas of the brain (Smith et al., 2012). T1 images were segmented in 5 tissue-types and registered to the preprocessed dMRI by means of FSL. For each participant, 1 million streamlines were generated seeding from the grey-matter/white-matter boundary using the iFOD2 probabilistic algorithm (Tournier, Calamante, & Connelly, 2010). Back-tracking option was applied in order to truncate streamlines terminating in anatomically implausible regions and re-tracking them to more adequate ending points (Smith et al., 2012). Finally, spherical-

Table 1

Descriptive statistics of Demographic, Cognitive, and Linguistic measures. Mean, standard deviation (SD) and range for each measure are reported. Raven's matrices raw scores are corrected according to participants' age and years of education; corrected scores range from 0 to 36 (cut-off = 18). Scores of the Test Breve di Intelligenza range from 0 to 50. BSWQ = Bilingual Switching Questionnaire; L1s = L2 > L1 switching tendencies; L2s = L1 > L2 switching tendencies; CS = contextual switching; US = unintended switching.

	Mean (SD)	Range
Age (years)	25.27 (4)	18–38
Education (years)	17.16 (1.86)	13–21
Annual family income (score)	3.59 (1.11)	1–5
L2 Age of Acquisition (AoA)	7.65 (3.46)	3–19
L2 Exposure (hours per day)	4.65 (3.55)	0–14
Translation task (L1 > L2) (% correct responses)	57.29 (3.94)	19–89
Cambridge Test (score)	18.26 (3.35)	9–25
BSWQ L1s (score)	6.92 (1.74)	3–10
BSWQ L2s (score)	9.19 (1.58)	4–13
BSWQ CS (score)	6.84 (2.62)	3–15
BSWQ US (score)	7.95 (1.30)	5–11
Raven's Matrices (corrected score)	31–37 (2.79)	26–36
Test Intelligenza Breve (score)	47.24 (2.15)	38.5–50

DWI

Fig. 1. Diffusion MRI preprocessing and analyses: a) Diffusion Weighted Images (DWI) are denoised, corrected for motion and distortions, and modeled with Multi-Shell Multi-Tissue Constrained Spherical Deconvolution; b) T1 Weighted (T1w) images are registered to processed DWI images, and Anatomically Constrained Tractography is performed to generate a 1 milion streamlines tractogram; c) T1w images are segmented with Freesurfer, and the Desikan/Killiany atlas parcellation is used to generate each participant's connectivity matrix; d) Network-Based Statistics (NBS) is adopted, and graph theoretical measures are extracted from the significant connected components.

a) DWI correction and Constrained Spherical Deconvolution

T1w

b) Anatomically Constrained Tractography

c) Brain parcellation and Connectome construction

d) Network-Based Statistics and Graph Theory

deconvolution informing filtering of tractograms (SIFT2) (Smith, Tournier, Calamante, & Connelly, 2015) was performed to correct for potential biases in overestimation of longer streamlines in CSD tractography while concurrently retaining the entire generated tractogram (i.e., a weight parameter is associated to each streamline, thus avoiding the need to remove some of them).

2.5. Connectome Construction

Connectivity matrices permitted the reduction of the brain's complexity to a simpler structure that represents the strength of the structural connectivity between all the regions that are part of a brain parcellation. For each participant, T1-weighted images were segmented with Freesurfer (v6.0.0, http://surfer.nmr.mgh.harvard.edu/) (Fischl, 2012). Cortical, cerebellar and subcortical structures were parcellated

into 84 distinct regions based on the Desikan/Killiany atlas (included bilateral subcortical regions: thalamus, caudate nucleus, putamen, pallidum, hippocampus, amygdala, nucleus accumbens) (Desikan et al., 2006). Brain parcellation was registered to each participant's tractogram in diffusion space, and 84x84 symmetric, weighted, undirected connectivity matrices were generated based on streamline count scaled by regional volume (Hagmann et al., 2008).

2.6. Statistical analyses

2.6.1. Correlation analyses between linguistic, demographic and cognitive measures

Preliminary statistical analyses were run to check for multi-collinearity between the following measures: Age, (years of formal) Education, L2 AoA, L2 Exposure, L1-to-L2 Translation Test, Cambridge

Test, and TIB. A Pearson's correlation coefficient was computed for each pair of measures. When variables were not normally distributed (as revealed by Kolmogorov-Smirnov test), Spearman's correlations were performed. When the correlation between two variables was high (r > 0.50, e.g., Taylor, 1990), only one of them was included in subsequent analyses. Age and Education were significantly correlated ($r_s = 0.57$; p < 0.001), hence only Education was included in the model. L1-to-L2 Translation Test and Cambridge Test scores were highly correlated ($r_s = 0.75$; p < .001). Since the Cambridge Test was also more significantly correlated with L2 Exposure than the Translation Test ($r_s = 0.46$; p < .001), the latter was preferred as a measure representative of participants' L2 Proficiency (the correlation matrix is reported in Supplementary Materials). No other measure was excluded from subsequent analyses. Analyses were performed with SciPy (Virtanen et al., 2020).

2.6.2. Network-based Statistic (NBS) analyses

The effects of distinct dual-language experiential factors on the brain's structural connectome were computed by means of the Network-based Statistic (NBS) Connectome toolbox (v 1.2; Zalesky, Fornito, & Bullmore, 2010) running on Matlab (v. 2019a). NBS is a validated nonparametric statistical method that permits the identification of which structural connections are affected by specific effects of interest in large networks (e.g., psychiatric pathologies, brain lesions, experience-induced brain plasticity, etc.). The assumption behind NBS is that such effects are rarely confined to a single connection and typically encompass multiple nodes forming interconnected subnetworks in the topological space (Fornito et al., 2016). NBS requires the statistical model to be specified as a general linear model (GLM). Therefore, each participant's 84×84 connectivity matrix was entered into GLM as the dependent variable, along with the following regressors: Gender, (years of formal) Education, L2 AoA, L2 Exposure, L2 Proficiency (Translation Test score), TIB, and model intercept. A multiple regression analysis was performed, testing for effects of L2 AoA, Exposure and Proficiency. First, NBS tests the same hypothesis at each and every possible network edge (connectome-wide analysis), so that each network's edge has a given test statistic value associated to it. A user-defined test statistic threshold is then applied to each edge and only the supra-threshold connections are kept (note that the choice of this threshold value affects the specificity, but not the sensitivity of the NBS method; see Fornito et al., 2016). Following NBS recommendations, network-forming threshold values were selected in order to balance network extension (avoiding an excessive number of connections) and effect strength (see Zalesky et al., 2010). Subsequently, NBS performs a form of clustering on the surviving edges by finding connected graph components in the topological space (which are the equivalent of clusters of pixels or voxels in physical space in fMRI mass univariate analyses). A connected component can be defined as a network structure in which a path always exists between any two nodes. For each component, a network Intensity measure was computed by summing the test values of each of the connections included in the component. With respect to other simpler measures such as network Extent (i.e., the total number of connections of a connected component), Intensity accounts for variations in effect sizes associated with each edge (similarly to Cluster Mass measure, see Bullmore et al., 1999). Moreover, Intensity is suited to precisely detect strong, focal effects associated with connectivity strength. Family Wise Error Rate (FWER) multiple comparison correction was applied to each generated connected component using permutation testing with 5,000 permutations (FWER corrected p-value < 0.05). Two outputs are provided by NBS analyses: significant effect-related connected components (i.e., effect-related subnetworks) and FWER corrected p-values associated to each component.

2.6.3. Graph theory Metrics of NBS Connected Components

Graph theory allows to estimate the topological properties of complex systems of interacting elements formed by nodes and edges such as brain networks (Fornito et al., 2016). Two analyses were performed in the graph theoretical framework. First, a set of measures was computed to better understand the organization of networks associated with specific dual-language experiential factors resulting from the NBS analyses. A weighted undirected adjacency matrix was computed for each significant effect-related connected component, with edges' weight corresponding to the t-values associated with the investigated effects. For each of these matrices, the following measures were estimated:

- *Node Degree*. Node degree is possibly the simplest measure in the graph theory framework and corresponds to the number of connections of each node (Fornito et al., 2016). The higher the degree, the higher the number of edges associated to a node. Node degree computation ignores edge weights.
- *Betweenness Centrality*. Betweenness centrality measures the proportion of all possible shortest paths (i.e., the minimum number of edges required to link any couple of nodes of a network) containing a given node (Brandes, 2001). The higher the betweenness centrality of a node, the more the node participates in a large number of shortest paths influencing other nodes (Freeman, 1978). Edge weights were considered in Betweenness Centrality computation (Brandes, 2001).
- *Modularity*. Most of the brain networks and subnetworks have a modular structure (Bullmore & Sporns, 2012). The Louvain method for community detection divides a given network into non-overlapping groups of nodes (or "communities") by maximizing the number of within-group connections and minimizing the number of between-group connections (Blondel, Guillaume, Lambiotte, & Lefebvre, 2008). This method allows one to investigate areas of segregation and specialization of information processing within a brain network. Edge weights were considered in Modularity computation (Blondel et al., 2008). Finally, all graph theoretical measures were computed with the Brain Connectivity Toolbox (BCT) (Rubinov & Sporns, 2010).

2.6.4. Whole-Connectome Graph Analysis

A second analysis was performed by comparing graph theoretical measures of the significant effect-related connected components from NBS with the same measures computed at the whole brain level. The aim of this analysis was to understand how the whole brain connectivity matrix is altered by the properties of effect-related subnetworks associated to dual language experiential factors. The previously estimated effect-related adjacency matrices were binarized, and edge values were substituted with each participant's connectivity value for that edge, in order to obtain a participant-specific effect-related connected component. The following measures were estimated for both the whole brain connectomes and the effect-related connected components:

- *Global Efficiency (Eglob)*. Global Efficiency is the average of the inverse shortest path length between each node and all other nodes in the network (Latora & Marchiori, 2001), and corresponds to a measure of connectome integration and inter-connectedness. The larger the Eglob value, the easier brain regions communicate with each other and specialized information is combined from all parts of the connectome (Rubinov & Sporns, 2010). Edge weights were considered in Eglob computation (Rubinov & Sporns, 2010).
- *Local Efficiency (Eloc)*. Local efficiency (Latora & Marchiori, 2001) is related to clustering measures and reflects the global efficiency computed on the neighborhood of a given node. In other words, local efficiency is the extent of the integration of a sub-graph consisting of only the nodes surrounding a certain node. Edge weights were considered in Eloc computation (Rubinov & Sporns, 2010).

Eglob and Eloc were computed with the Brain Connectivity Toolbox (BCT) (Rubinov & Sporns, 2010). Correlation analyses between the efficiency of connected components and that of the whole brain network were performed by means of the Robust Correlation Toolbox (Pernet, Wilcox, & Rousselet, 2013).

2.6.5. Correlation analyses between efficiency measures and switching tendencies

Finally, global and local efficiency measures estimated from the effect-related subnetworks were also correlated with the BSWQ scores, in order to investigate the relationship between the efficiency of effect-related connected components and each participant's self-reported switching tendencies.

3. Results

3.1. Network-based Statistics (NBS) analyses

For each significant connected component, graph theoretical metrics are also reported.

- L2 AoA. No significant effect was found.
- L2 Exposure. NBS analyses revealed two connected components associated with a significant effect of L2 Exposure (primary component-forming T-threshold = 3.6). The first component (FWER

corrected p-value = 0.025) is a large temporo-parieto-occipital network involving brain regions in both hemispheres (see Tables 2 and 3, Fig. 2). Graph theoretical measures revealed three modules: i) A module centred around the left superior temporal sulcus, including left medial temporal regions (hippocampal, parahippocampal and entorhinal cortices), the left amygdala, and the left supramarginal gyrus; ii) temporo-parieto-occipital regions centred around the left paracentral lobule and the fusiform gyrus, including the lateral occipital cortex, the inferior parietal lobule, and the right pallidum and iii) temporo-parieto-occipital regions centred around the right paracentral lobule, including the isthmus of the right cingulate cortex, the right precentral gyrus, and the left lingual gyrus.

The second connected component (FWER corrected p-value = 0.049) consists of a left-sided subnetwork involving fronto-opercular and cingulate cortices (see Tables 2 and 3, Fig. 3). Graph theory showed a modular structure: i) A module centred around the anterior cingulate cortex and encompassing the insular cortex and the caudal part of the middle frontal gyrus; ii) a second module centred around the medial

Table 2

Graph theoretical measures associated with significant effect-related connected components. AoA = Age of Acquisition. Anatomical labels from the Desikan-Killany Atlas are adopted; lh = left hemisphere; rh = right hemisphere.

Network	Node (Desikian-Killany labels)	Node Degree	Betweenness Centrality	Module (Louvain community)
Exposure I	lh-banksts	5	108	1
Exposure I	lh-fusiform	3	110	2
Exposure I	lh-paracentral	3	106	2
Exposure I	rh-paracentral	3	70	3
Exposure I	lh-entorhinal	2	26	1
Exposure I	lh-inferiorparietal	2	80	2
Exposure I	rh-isthmuscingulate	2	26	3
Exposure I	lh-lateraloccipital	1	0	2
Exposure I	lh-lingual	1	0	3
Exposure I	lh-parahippocampal	1	0	1
Exposure I	lh-supramarginal	1	0	1
Exposure I	lh-hippocampus	1	0	1
Exposure I	lh-amygdala	1	0	1
Exposure I	rh-pallidum	1	0	2
Exposure I	rh-precentral	1	0	3
Exposure II	lh-medialorbitofrontal	3	28	2
Exposure II	lh-rostralanteriorcingulate	3	22	1
Exposure II	lh-lateralorbitofrontal	2	12	3
Exposure II	lh-parsopercularis	2	24	2
Exposure II	lh-caudalmiddlefrontal	1	0	1
Exposure II	lh-parstriangularis	1	0	2
Exposure II	lh-superiorfrontal	1	0	3
Exposure II	lh-insula	1	0	1
Proficiency	lh-rostralmiddlefrontal	4	48	1
Proficiency	lh-superiortemporal	4	48	2
Proficiency	rh-superiorparietal	4	87	4
Proficiency	lh-precuneus	3	58	3
Proficiency	lh-hippocampus	2	22	3
Proficiency	rh-precuneus	2	9	1
Proficiency	lh-isthmuscingulate	1	0	2
Proficiency	lh-temporalpole	1	0	3
Proficiency	lh-putamen	1	0	1
Proficiency	rh-hippocampus	1	0	3
Proficiency	rh-inferiorparietal	1	0	2
Proficiency	rh-paracentral	1	0	1
Proficiency	rh-precentral	1	0	4
Exposure*AoA	lh-caudalmiddlefrontal	6	94	1
Exposure*AoA	lh-middletemporal	1	0	2
Exposure*AoA	lh-parsopercularis	1	0	2
Exposure*AoA	lh-superiorfrontal	1	0	2
Exposure*AoA	rh-thalamus-proper	2	20	3
Exposure*AoA	rh-putamen	1	0	1
Exposure*AoA	rh-pallidum	1	0	1
Exposure*AoA	rh-hippocampus	1	0	1
Exposure*AoA	rh-caudalanteriorcingulate	1	0	3
Exposure*AoA	rh-caudalmiddlefrontal	4	54	2
Exposure*AoA	rh-precentral	2	20	4
Exposure*AoA	rh-supramarginal	1	0	4

Table 3
Test values associated with the edges of the Exposure I and Exposure II connected components. Anatomical labels from the Desikan-Killany Atlas are adopted; lh = left hemisphere; rh = right hemisphere.

Node i (Desikan-Killiany labels)	Node j (Desikan-Killiany labels)	T-Value
Exposure I		
lh-banksts	lh-entorhinal	4.78
lh-banksts	lh-fusiform	3.83
lh-banksts	lh-parahippocampal	3.91
lh-fusiform	lh-paracentral	3.82
lh-inferiorparietal	lh-paracentral	3.88
lh-lateraloccipital	lh-paracentral	4.13
lh-entorhinal	lh-supramarginal	3.64
lh-banksts	lh-hippocampus	4.41
lh-banksts	lh-amygdala	4.63
lh-fusiform	rh-pallidum	3.86
lh-inferiorparietal	rh-paracentral	3.66
lh-lingual	rh-paracentral	4.44
rh-isthmuscingulate	rh-paracentral	3.78
rh-isthmuscingulate	rh-precentral	3.63
Exposure II		
lh-lateralorbitofrontal	lh-medialorbitofrontal	3.75
lh-medialorbitofrontal	lh-parsopercularis	4.07
lh-medialorbitofrontal	lh-parstriangularis	4.44
lh-caudalmiddlefrontal	lh-rostralanteriorcingulate	4.10
lh-parsopercularis	lh-rostralanteriorcingulate	3.92
lh-lateralorbitofrontal	lh-superiorfrontal	4.54
lh-rostralanteriorcingulate	lh-insula	3.72

orbitofrontal cortex, including the pars orbitalis and triangularis of the inferior frontal gyrus and iii) a third module consisting of the lateral orbitofrontal cortex and the superior frontal gyrus.

- *L2 Proficiency.* NBS analyses revealed an extensive connected component associated with a significant effect of L2 Proficiency (primary component-forming T-threshold = 2.85; FWER corrected p-value = 0.046). This subnetwork consisted mainly of fronto-temporal, parietal, but also subcortical regions distributed across the two hemispheres (see Tables 2 and 4, Fig. 4). Graph theory showed the presence of four connected modules: i) A first module centred around the rostral part of the left middle frontal gyrus and

encompassing the right paracentral lobule, the right precuneus and the left putamen; ii) a second module centred around the left superior temporal gyrus, involving the right inferior parietal lobule and the isthmus of the left cingulate cortex; iii) a third module centred around the left precuneus and involving the bilateral hippocampi and the left temporal pole and iv) a fourth model, connecting modules i) and ii) with module iii), and consisting of the right superior parietal cortex (highest betweenness centrality) and the right precentral gyrus.

- *L2 AoA × L2 Exposure.* NBS analyses revealed a fronto-temporal and subcortical connected component resulting from a significant interaction between L2 AoA and L2 Exposure (primary component-forming T-threshold = 2.7; FWER corrected p-value = 0.018). Graph theoretical measures showed a central role played by the bilateral caudal parts of the middle frontal gyrus, which were directly connected to each other. Four interconnected modules were found: i) A module centred on the caudal part of the left middle frontal gyrus, connected with contralateral subcortical structures (putamen and pallidum) and the right hippocampus; ii) a module consisting of the caudal part of the right middle frontal gyrus, connected with contralateral temporo-frontal cortices (middle temporal gyrus, superior frontal gyrus and pars opercularis of the inferior frontal gyrus); iii) and iv) peripheral modules respectively centred around the right thalamus (connecting the anterior cingulate cortex) and the right precentral gyrus (connecting the right supramarginal gyrus) (see Table 2 and 5, Fig. 5).

No significant effect was found for *L2 AoA × L2 Proficiency*, and *L2 Proficiency × L2 Exposure* interactions.

3.2. Whole-Connectome Graph Analysis

Given the absence of triplets of nodes surrounding any node of the significant connected components, it was not possible to compute the Local Efficiency (Eloc) measure for the effect-related subnetworks. Hence, only Global Efficiency (Eglob) was used in the analyses for the connected components, whereas for the whole-brain efficiency both Eglob and Eloc were considered. Significant positive correlations were found between the global efficiency of the L2 proficiency connected
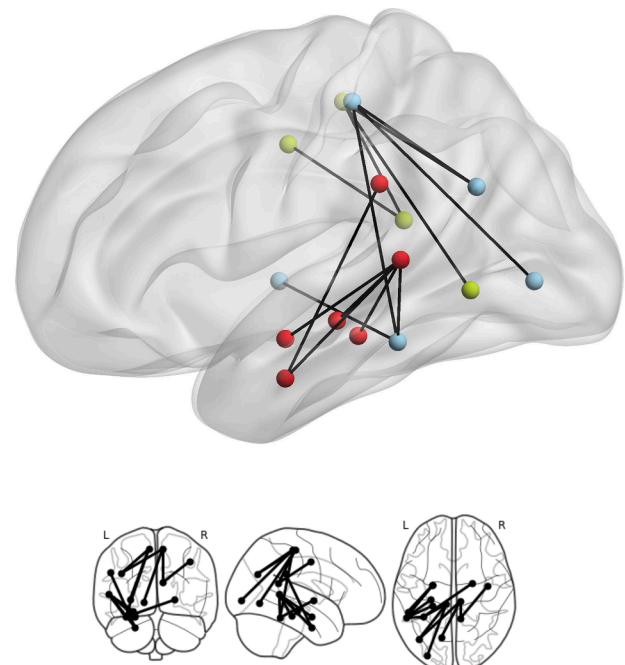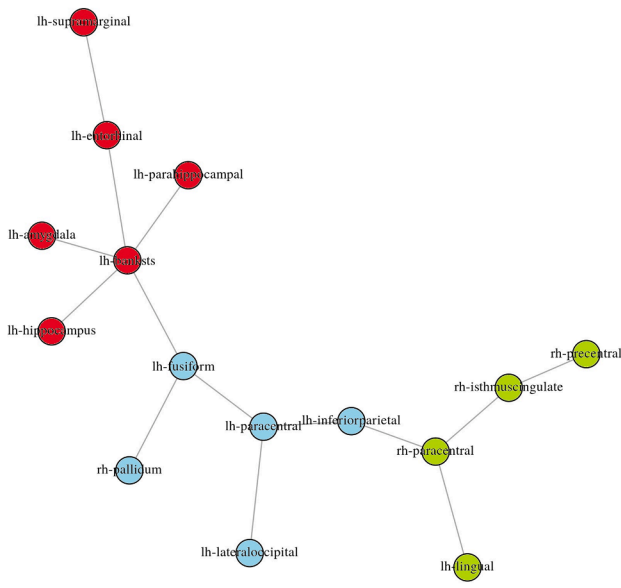
Fig. 2. L2 Exposure I connected component. lh = Left Hemisphere; rh = Right Hemisphere.
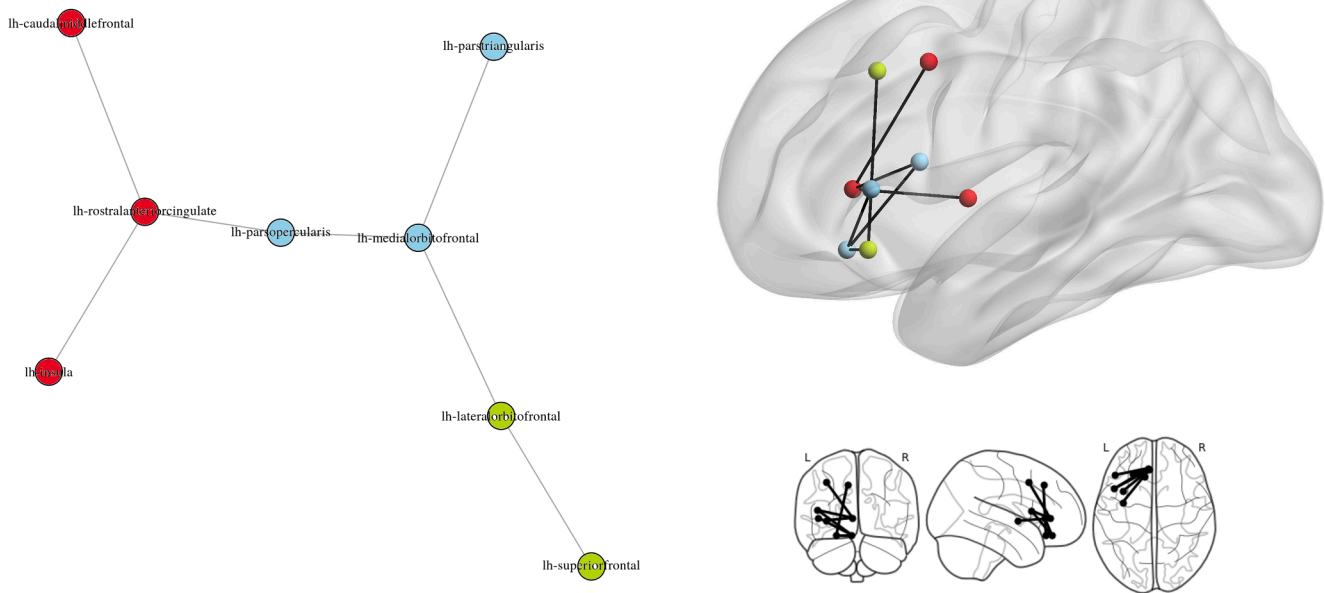
Fig. 3. L2 Exposure II connected component. lh = Left Hemisphere; rh = Right Hemisphere.

Table 4
Test values associated with the edges of the Proficiency connected component. Anatomical labels from the Desikan-Killiany Atlas are adopted; lh = left hemisphere; rh = right hemisphere.

Node i (Desikan-Killiany labels)	Node j (Desikan-Killiany labels)	T-Value
lh-isthmuscingulate	lh-superiortemporal	2.93
lh-rostralmiddlefrontal	lh-putamen	2.87
lh-precuneus	lh-hippocampus	3.18
lh-temporalpole	lh-hippocampus	3.25
lh-precuneus	rh-hippocampus	3.15
lh-superiortemporal	rh-inferiorparietal	3.07
lh-rostralmiddlefrontal	rh-paracentral	3.39
lh-rostralmiddlefrontal	rh-precuneus	3.20
lh-superiortemporal	rh-precuneus	3.05
lh-precuneus	rh-superiorparietal	2.88
lh-rostralmiddlefrontal	rh-superiorparietal	3.23
lh-superiortemporal	rh-superiorparietal	3.53
rh-precentral	rh-superiorparietal	2.95

component and the Eglob ($r_s = 0.69$; p < .001) and Eloc ($r_s = 0.65$; p < .001) efficiency measures of the whole brain network. Similarly, the global efficiency of the connected component associated with the Exposure by AoA interaction was significantly correlated with the global ($r_s = 0.38$; p < .001) and local ($r_s = 0.43$; p < .001) efficiency of the whole brain.

3.3. Correlation between efficiency measures and switching tendencies

A significant correlation was found between the Eglob measure of the L2 AoA × L2 Exposure interaction connected components and the BSWQ Unintended Switching score ($r_s = -0.24$; p < 0.05).

4. Discussion

Recall that the present study aimed at defining the distinct contribution of bilingual experiential factors in shaping the brain structural connectome. Whole-brain probabilistic tractography was performed and a Network Based Statistics approach was adopted to identify networks of regions in which structural connectivity was significantly modulated by L2 Exposure, L2 Proficiency, and L2 AoA. Graph theoretical measures

were collected to further explore whether whole-brain interconnectedness was altered by the properties of these networks. In the following, we discuss the distinct anatomical organization and topological properties of each of the connected components, and the general implications of our findings.

4.1. Exposure – Subnetwork I (posterior)

The first connected component consists of a temporo-parieto-occipital network. Recall that graph theoretical measures revealed a central role played by the posterior part of the left superior temporal sulcus (STS) (highest nodal degree and high betweenness centrality). Under the dual stream model of speech processing by Hickok and Poeppel (2000, 2004, 2016), the STS communicates with temporal areas responsible for phonological to conceptual mapping, mediating lexical access. In our analysis, STS was found to be directly connected with the ventromedial temporal lobe (i.e., fusiform, lingual, entorhinal, and parahippocampal gyri, and hippocampus), a region highly involved in semantic processing (Hoenig & Scheef, 2005) and vocabulary learning (Bellander et al., 2016; Breitenstein et al., 2005; see also Davis & Gaskell, 2009). In sum, this area seems to be critical for the acquisition, maintenance, and retrieval of lexico-semantic information.

Our findings suggest that L2 exposure modulates and reinforces connections between a network of regions along the left ILF that are central to phonological-to-semantic mapping. This interpretation is compatible with the findings of Kuhl et al. (2016), who reported significant correlations between microstructural properties of the ILF and the amount of L2 exposure, weighted by linguistic immersion (i.e. duration of residence in a foreign country). We found that the STS was also indirectly connected with parietal areas such as the left inferior parietal lobule and the supramarginal gyrus, most likely through the SLF/AF in the dorsal stream. In line with this result, Sulpizio, Del Maschio, Del Mauro et al. (2020), reported greater functional connectivity within parietal regions as a factor of increased L2 exposure, especially in late bilinguals.

Moreover, the Adaptive Control hypothesis (Green & Abutalebi, 2013) includes these implicated areas in a network of regions that sustain context-dependent language selection and monitor speech production in bilinguals. While parietal regions have been suggested to be
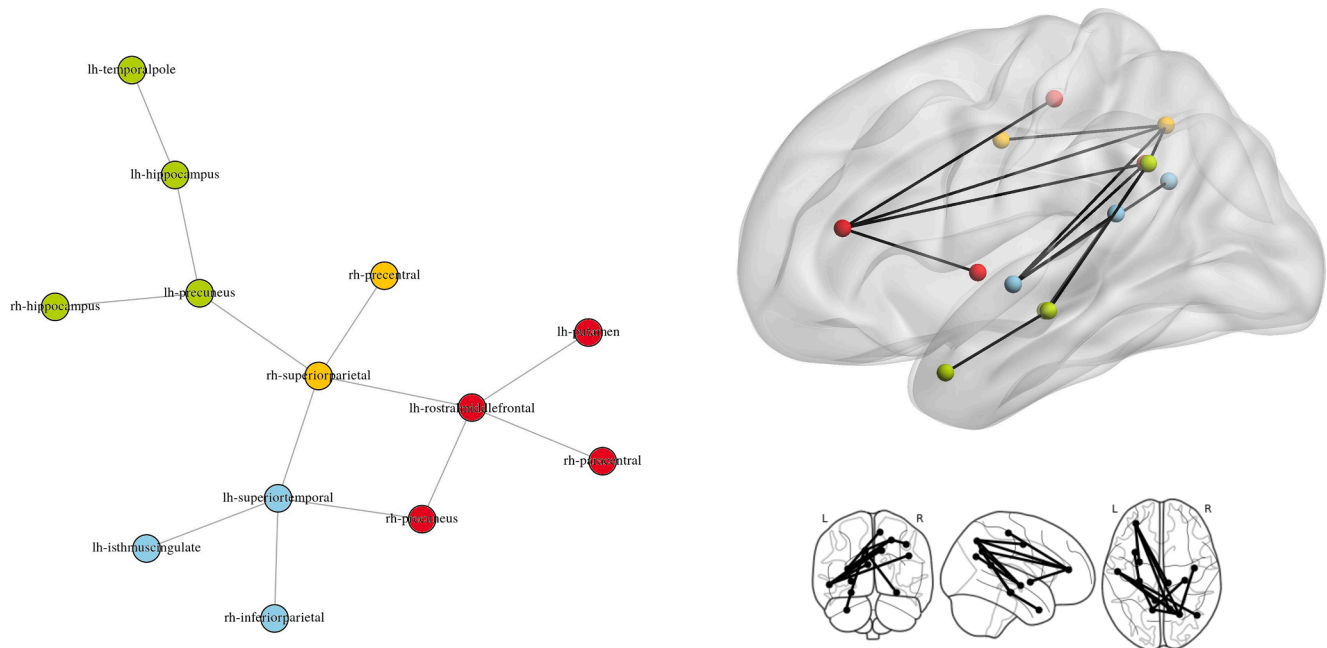
Fig. 4. L2 Proficiency connected component. lh = Left Hemisphere; rh = Right Hemisphere.

Table 5
Test values associated with the edges of the Exposure*Age of Acquisition interaction connected components. Anatomical labels from the Desikan-Killany Atlas are adopted; lh = left hemisphere; rh = right hemisphere.

Node i (Desikan-Killiany labels)	Node j (Desikan-Killiany labels)	T-Value
lh-caudalmiddlefrontal	rh-thalamus-proper	2.93
lh-caudalmiddlefrontal	rh-putamen	2.84
lh-caudalmiddlefrontal	rh-pallidum	3.23
lh-caudalmiddlefrontal	rh-hippocampus	3.04
rh-thalamus-proper	rh-caudalanteriorcingulate	2.70
lh-caudalmiddlefrontal	rh-caudalmiddlefrontal	3.68
lh-middletemporal	rh-caudalmiddlefrontal	2.98
lh-parsopercularis	rh-caudalmiddlefrontal	2.74
lh-superiorfrontal	rh-caudalmiddlefrontal	3.32
lh-caudalmiddlefrontal	rh-precentral	2.71
rh-precentral	rh-supramarginal	2.74

relevant in sensory-motor integration, allowing the detection and correction of speech errors (Buchsbaum et al., 2011; Hickok & Poeppel, 2016) as well as the storing of lexico-semantics representations (see the "Dual Lexicon" model by Gow, 2012; Gold, Powell, Xuan, Jiang, & Hardy, 2007), here we limit ourselves to highlighting their role for language selection and maintenance. Based on these considerations, we suggest that L2 exposure modulates the connectivity within a set of regions in "Subnetwork I", which sustain aspects of speech comprehension via the ventral stream and language selection through the dorsal stream.

4.2. Exposure – Subnetwork II (anterior)

The second connected component consists of a left-hemispheric network involving fronto-opercular and cingulate cortices, possibly connected by short-range intragyral U-fibers and the left IFOF. The pars opercularis (Brodmann area 44) and triangularis (Brodmann area 45) of the left inferior frontal gyrus are well known to play a central role in speech production and syntactic processing (Friederici, 2009; Haagort, 2005; Hickok & Poeppel, 2004). Several functional neuroimaging studies have reported shared inferior frontal activations for both first and second language processing in bilingual individuals (for an overview, see Sulpizio, Del Maschio, Fedeli, & Abutalebi, 2020). The pars opercularis, a region with one of the highest centrality scores within this

network, was also directly connected with a module including the left insula, the anterior cingulate cortex, and the middle frontal gyrus. Not only does the anterior insula actively contribute to speech production and articulation (Ardila, Bernal, & Rosselli, 2014; Oh, Duerden, & Pang, 2014), but it is also relevant for dual-language switching in bilinguals by controlling verbal interference during word retrieval and articulation (Parker Jones et al., 2012). The anterior cingulate cortex is a key region for monitoring both linguistic and cognitive conflicts (Botvinick, Braver, Barch, Carter, & Cohen, 2001; Luk, Green, Abutalebi, & Grady, 2012). This region has been proposed to act as a supervisory attentional system in bilingual language control, which is required during language switching (Branzi, Della Rosa, Canini, Costa, & Abutalebi, 2016). Moreover, several accounts of preserved gray matter volume in this region with increasing age support that the ACC incurs in neuroplastic changes as a consequence of bilingual experience (Abutalebi et al., 2015; Del Maschio, Fedeli, Sulpizio, & Abutalebi, 2019; see also Del Maschio, Sulpizio et al., 2019). And finally, in this network, the middle and superior frontal gyri are part of the dorsolateral prefrontal cortex, a region that is responsible for resolving conflicts by controlling interfering linguistic information (Branzi et al., 2016; Calabria et al., 2018).

Based on the results of Subnetwork II, we suggest that L2 exposure reinforces a WM network that connects regions crucial for speech production and articulation, actively monitored by executive areas. Increased L2 exposure would prompt enhanced frontal connectivity with domain-general executive regions because of the intensification of language-control demands. This interpretation is in line with the Dynamic Reconstruction Model of Pliatsikas (2020). The model argues for IFOF adaptation and increased control efficiency as a function of L2 exposure/immersion. Notably, in a structural connectivity study comparing Spanish monolinguals and early Spanish-Basque bilinguals, García-Pentón et al. (2014) reported a very similar left-hemispheric subnetwork. Thus, our findings expand previous knowledge about this subnetwork by revealing that the connectivity within its regions is modulated by L2 exposure.

4.3. Proficiency

L2 proficiency affected a network of parietal, frontal, and temporal regions distributed with a rostrocaudal gradient across the two
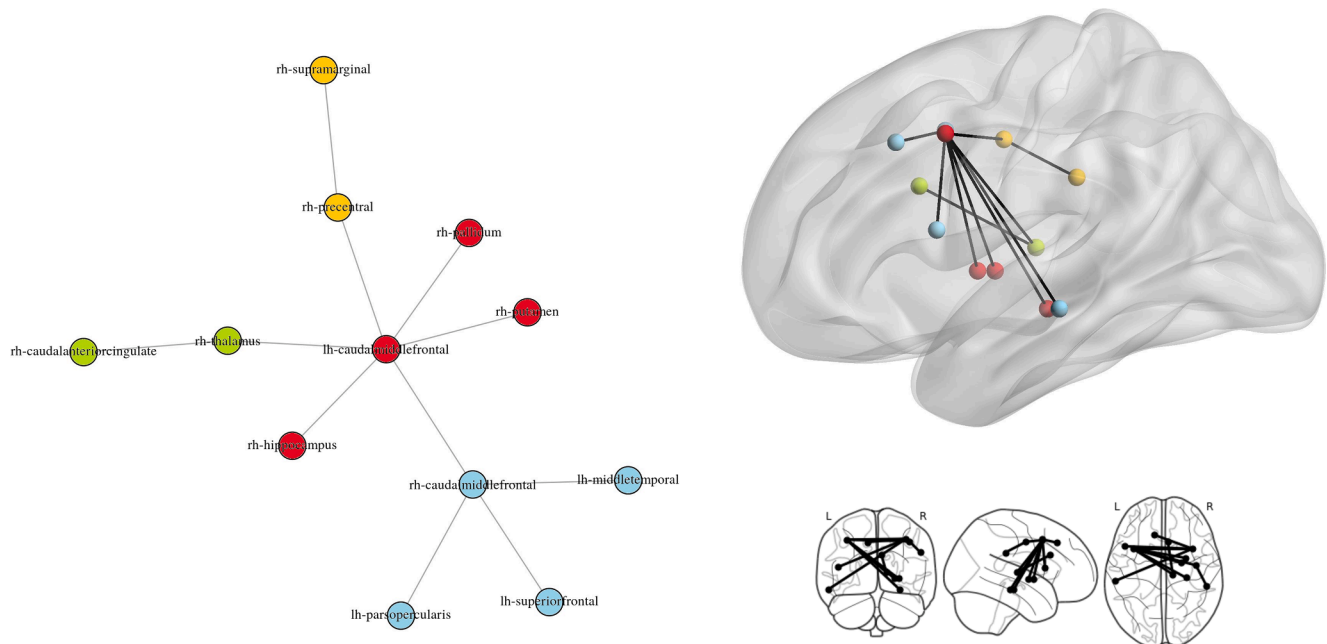
Fig. 5. L2 Age of Acquisition * Exposure connected component. lh = Left Hemisphere; rh = Right Hemisphere.

hemispheres. In the most rostral module, the left middle frontal gyrus was connected with the left putamen. According to the Adaptive Control hypothesis (Green & Abutalebi, 2013), fronto-putaminal connections participate in the bilingual language control network, and the middle frontal gyrus, which corresponds to the dorsolateral prefrontal cortex, is involved in conflict resolution (see Exposure Subnetwork II). Moving posteriorly, in the medial temporal lobe, the hippocampal contribution is shared with the Exposure Subnetwork I. Both this region and the left temporal pole are of crucial importance for storing lexico-semantic representations and sustaining L2 vocabulary learning in bilinguals (Li et al., 2017; Stein et al., 2012), while the left superior temporal gyrus participates in speech perception and comprehension (2016; Hickok & Poeppel, 2004). The most caudal portion of the network consisted of multiple interconnected parietal regions. The inferior parietal lobule has been proposed to underpin the acquisition of sensorimotor patterns when learning novel words (Lee et al., 2007; Mechelli et al., 2004) and the maintenance of language representations during bilingual language production to achieve correct language output. (Abutalebi & Green, 2008). Brain lesions involving this region have been frequently associated with pathological forms of language selection and switching behavior in bilingual individuals (Leischner, 1987; Pötzl, 1925). Moving dorsally, the superior parietal lobule constitutes the topological centre of the network (highest nodal degree and betweenness centrality) and participates in the dorsal attention network (DAN). The DAN consists of a group of fronto-parietal regions that regulate top-down voluntary attention orienting and stimuli selection (Corbetta & Shulman, 2002). These functions are essential for efficient language switching, as revealed by several accounts of parietal activity during mixed-language picture naming tasks (De Baene, Duyck, Brass, & Carreiras, 2015; Reverberi et al., 2015). Moreover, Consonni et al. (2013) showed that the right superior parietal lobule and the bilateral precuneus were functionally active in native and non-native language verb and noun production in bilinguals. Based on these accounts, we suggest that L2 proficiency modulates the connectivity within a network of regions that sustain vocabulary acquisition and L2 learning. Inside this network, frontoparietal nodes would represent a language selection system that is connected with regions crucial for lexico-semantic representation in the temporal lobe. With higher L2 proficiency, stronger fronto-parietal connectivity would lead to an efficient attention direction to the language necessary to access and store lexico-semantic representations.

This interpretation is compatible with the results of previous cross-sectional and longitudinal DTI-based studies reporting higher FA in the right fronto-temporo-parietal white matter (e.g. SLF/AF) as a function of L2 proficiency and word learning (Hosoda et al., 2013; Nichols & Joanisse, 2016). Similar results were also found by Sulpizio, Del Maschio, Del Mauro et al. (2020), who reported increased superior temporal gyrus/precuneus/temporal pole functional connectivity associated with greater proficiency in late bilinguals. Consistent with our interpretation, the authors suggested that this connection would sustain attention orientation to the lexical representations of the to-be-used language.

Graph theoretical measures showed that as global efficiency increases in this network (i.e. it becomes more interconnected), both local and global efficiency increase in the whole-brain connectome. This result is in contrast to that of García-Pentón et al. (2014), who reported decreased whole-brain efficiency in the face of greater subnetworks global efficiency in bilinguals. The difference may possibly be ascribed to the different conceptualization of bilingualism in the two studies (binary *vs* multi-factorial gradient,) which leads to two non-overlapping networks with distinct topological properties. In fact, relative to the results of García-Pentón and colleagues, our proficiency-modulated network exhibits a larger number of nodes and inter-hemispheric connections. In a structural connectomic study, Owen et al. (2013) have shown that inter-hemispheric callosal connections play a critical role in modulating whole-brain efficiency, allowing long-range information transmission between distant connectivity hubs. Our result indicates that L2 proficiency is beneficial to the brain small-world organization, which is efficient information integration over a range of scales (local and global) in the face of relatively low wiring cost (Fornito et al., 2016; Latora & Marchiori, 2001).

4.4. Interaction between AoA and Exposure

The interaction between L2 AoA and exposure led to a bilateral network centred on frontal regions and including subcortical and temporo-parietal areas. At the core of the network, the bilateral middle frontal gyri were directly connected to each other, and with contralateral brain regions. The right middle frontal gyrus was connected with the left middle temporal gyrus, and the inferior, middle, and superior frontal gyri. This result indicates a modulation of the connectivity of the

right dorsolateral prefrontal cortex with contralateral language regions crucial for comprehension, production, and monitoring. The left middle frontal gyrus was connected with the contralateral middle frontal gyrus, right-hemispheric parietal cortex, and subcortical nuclei. These regions are important for lexico-semantic representation, conflict monitoring and language selection (Abutalebi & Green, 2016; Burgaleta, Sanjuán, Ventura-Campos, Sebastian-Galles, & Ávila, 2016; Mamiya, Richards, & Kuhl, 2018). Based on the inter-hemispheric structure of the network, we propose that AoA and Exposure affect the fronto-callosal connectivity, a result consistent with previous accounts of increased myelination in portions of the CC in bilingual individuals (DeLuca, Rothman, et al., 2019; Luk et al., 2011; Pliatsikas, Moschopoulou, & Saddy, 2015; Rahmani et al., 2017). Plots of the global efficiency values revealed that on low levels of L2 Exposure, early (AoA $\leq$ 6) and late (AoA $>$ 6) bilinguals showed similar levels of global efficiency. This network becomes more segregated (i.e. more local and less global efficient) in late L2 learners with increasing Exposure. Early bilinguals, instead, show maintained global efficiency with high L2 Exposure via a less steep slope. We suggest that late bilinguals rely on this network (and not on other structures) to face high levels of L2 exposure. In a recent study, Deluca, Rothman, et al. (2019), DeLuca, Rothman, et al. (2019) showed that the later an L2 is learned, the more bilinguals rely on fronto-callosal connectivity. Moreover, a subset of the same authors reported that CC myelination correlated with the length of L2 immersion (Deluca, Rothman, et al. (2019)), and suggested that both AoA and immersion should promote more efficient and instinctive language control. In our study, the global efficiency score of this network was negatively correlated with the Unintended Switching measure of the BSWQ, indicating that more segregation of this network is beneficial to language control. This is compatible with the findings of Bonfieni and colleagues (Bonfieni, Branigan, Pickering, & Sorace, 2019), who reported that the more an individual is exposed to an L2, the easier she/he switches between the native and non-native languages. On the other hand, early L2 acquisition may contribute to the development of broader WM interregional connectivity, and early bilinguals may rely on distinct pathways to deal with increasing linguistic demands associated with greater L2 exposure. Overall, this network well represents the dynamic nature of bilingual language control, which is influenced by multiple experiential factors across the lifespan such as L2 onset and the dynamic nature of Exposure.

5. Conclusion

In the present study, we used cutting-edge MRI diffusion processing techniques and network neuroscience as a methodological framework to investigate networks of regions in which structural connectivity was modulated by distinct bilingual experiential factors. L2 Exposure, L2 Proficiency, and L2 AoA (in interaction with Exposure) differentially affected the structural organization of linguistic pathways and the communication between regions relevant for language control. These results are in line with established brain models of dual-language representation and monitoring. Our study overcomes some methodological constraints of previous experiments and expands the knowledge about the neuroanatomical correlates of bilingual experience by providing new models of large-scale white matter organization in bilinguals.

Declaration of Competing Interest

The authors declare that they have no known competing financial interests or personal relationships that could have appeared to influence the work reported in this paper.

Appendix A. Supplementary material

Supplementary data to this article can be found online at https://doi.org/10.1016/j.bandl.2021.104978.

References

Abutalebi, J., & Green, D. (2007). Bilingual language production: The neurocognition of language representation and control. *Journal of Neurolinguistics, 20*, 242–275.

Abutalebi, J., & Green, D. W. (2008). Control mechanisms in bilingual language production: Neural evidence from language switching studies. *Language and Cognitive Processes, 23*(4), 557–582.

Abutalebi, J., & Green, D. W. (2016). Neuroimaging of language control in bilinguals: Neural adaptation and reserve. *Bilingualism: Language and Cognition, 19*(4), 689–698.

Abutalebi, J., Guidi, L., Borsa, V., Canini, M., Della Rosa, P. A., Parris, B. A., & Weekes, B. S. (2015). Bilingualism provides a neural reserve for aging populations. *Neuropsychologia, 69*, 201–210.

Andersson, J. L., & Sotiropoulos, S. N. (2016). An integrated approach to correction for off-resonance effects and subject movement in diffusion MR imaging. *Neuroimage, 125*, 1063–1078.

Andersson, J. L., Graham, M. S., Zsoldos, E., & Sotiropoulos, S. N. (2016). Incorporating outlier detection and replacement into a non-parametric framework for movement and distortion correction of diffusion MR images. *Neuroimage, 141*, 556–572.

Ardila, A., Bernal, B., & Rosselli, M. (2014). Participation of the insula in language revisited: A meta-analytic connectivity study. *Journal of Neurolinguistics, 29*, 31–41.

Bach, M., Laun, F. B., Leemans, A., Tax, C. M., Biessels, G. J., Stieltjes, B., & Maier-Hein, K. H. (2014). Methodological considerations on tract-based spatial statistics (TBSS). *Neuroimage, 100*, 358–369.

Basso, A., Capitani, E., & Laiacona, M. (1987). Raven's coloured progressive matrices: Normative values on 305 adult normal controls. *Functional Neurology, 2*, 189–194.

Bellander, M., Berggren, R., Mårtensson, J., Brehmer, Y., Wenger, E., Li, T. Q., … Lövdén, M. (2016). Behavioral correlates of changes in hippocampal gray matter structure during acquisition of foreign vocabulary. *Neuroimage, 131*, 205–213.

Blondel, V. D., Guillaume, J. L., Lambiotte, R., & Lefebvre, E. (2008). Fast unfolding of communities in large networks. *Journal of Statistical Mechanics: Theory and Experiment, 2008*(10), P10008.

Bonfieni, M., Branigan, H. P., Pickering, M. J., & Sorace, A. (2019). Language experience modulates bilingual language control: The effect of proficiency, age of acquisition, and exposure on language switching. *Acta Psychologica, 193*, 160–170. https://doi.org/10.1016/j.actpsy.2018.11.004.

Botvinick, M. M., Braver, T. S., Barch, D. M., Carter, C. S., & Cohen, J. D. (2001). Conflict monitoring and cognitive control. *Psychological Review, 108*(3), 624.

Brandes, U. (2001). A faster algorithm for betweenness centrality. *Journal of Mathematical Sociology, 25*(2), 163–177.

Branzi, F. M., Della Rosa, P. A., Canini, M., Costa, A., & Abutalebi, J. (2016). Language control in bilinguals: Monitoring and response selection. *Cerebral Cortex, 26*(6), 2367–2380.

Breitenstein, C., Jansen, A., Deppe, M., Foerster, A. F., Sommer, J., Wolbers, T., & Knecht, S. (2005). Hippocampus activity differentiates good from poor learners of a novel lexicon. *NeuroImage, 25*(3), 958–968.

Buchsbaum, B. R., Baldo, J., Okada, K., Berman, K. F., Dronkers, N., D'Esposito, M., & Hickok, G. (2011). Conduction aphasia, sensory-motor integration, and phonological short-term memory–an aggregate analysis of lesion and fMRI data. *Brain and Language, 119*(3), 119–128.

Bullmore, E. T., Suckling, J., Overmeyer, S., Rabe-Hesketh, S., Taylor, E., & Brammer, M. J. (1999). Global, voxel, and cluster tests, by theory and permutation, for a difference between two groups of structural MR images of the brain. *IEEE Transactions on Medical Imaging, 18*(1), 32–42.

Bullmore, E., & Sporns, O. (2009). Complex brain networks: Graph theoretical analysis of structural and functional systems. *Nature Reviews Neuroscience, 10*(3), 186–198.

Bullmore, E., & Sporns, O. (2012). The economy of brain network organization. *Nature Reviews Neuroscience, 13*(5), 336–349.

Burgaleta, M., Sanjuán, A., Ventura-Campos, N., Sebastian-Galles, N., & Ávila, C. (2016). Bilingualism at the core of the brain. Structural differences between bilinguals and monolinguals revealed by subcortical shape analysis. *NeuroImage, 125*, 437–445.

Calabria, M., Costa, A., Green, D. W., & Abutalebi, J. (2018). Neural basis of bilingual language control. *Annals of the New York Academy of Sciences, 1426*(1), 221–235.

Colombo, L., Sartori, G., & Brivio, C. (2002). Stima del quoziente intellettivo tramite l'applicazione del TIB (test breve di Intelligenza). *Giornale Italiano di Psicologia, 29*(3), 613–638.

Consonni, M., Cafiero, R., Marin, D., Tettamanti, M., Iadanza, A., Fabbro, F., & Perani, D. (2013). Neural convergence for language comprehension and grammatical class production in highly proficient bilinguals is independent of age of acquisition. *Cortex, 49*(5), 1252–1258.

Corbetta, M., & Shulman, G. L. (2002). Control of goal-directed and stimulus-driven attention in the brain. *Nature Reviews Neuroscience, 3*(3), 201–215.

Cummine, J., & Boliek, C. A. (2013). Understanding white matter integrity stability for bilinguals on language status and reading performance. *Brain Structure and Function, 218*(2), 595–601.

Davis, M. H., & Gaskell, M. G. (2009). A complementary systems account of word learning: Neural and behavioural evidence. *Philosophical Transactions of the Royal Society B: Biological Sciences, 364*(1536), 3773–3800.

De Baene, W., Duyck, W., Brass, M., & Carreiras, M. (2015). Brain circuit for cognitive control is shared by task and language switching. *Journal of Cognitive Neuroscience, 27*(9), 1752–1765.

Del Maschio, N., & Abutalebi, J. (2019). Language organization in the bilingual and multilingual brain. In J. W. Schwieter (Ed.), *The handbook of the neuroscience of multilingualism* (pp. 197–213). John Wiley & Sons.

Del Maschio, N., Fedeli, D., Sulpizio, S., & Abutalebi, J. (2019a). The relationship between bilingual experience and gyrification in adulthood: A cross-sectional surface-based morphometry study. *Brain and Language, 198*, Article 104680.

Del Maschio, N., Sulpizio, S., Fedeli, D., Ramanujan, K., Ding, G., Weekes, B. S., … Abutalebi, J. (2019b). ACC sulcal patterns and their modulation on cognitive control efficiency across lifespan: A neuroanatomical study on bilinguals and monolinguals. *Cerebral Cortex, 29*(7), 3091–3101.

Del Maschio, N., Sulpizio, S., Toti, M., Caprioglio, C., Del Mauro, G., Fedeli, D., & Abutalebi, J. (2019c). Second language use rather than second language knowledge relates to changes in white matter microstructure. *Journal of Cultural Cognitive Science*, 1–11.

Deluca, V., Rothman, J., & Pliatsikas, C. (2019). Linguistic immersion and structural effects on the bilingual brain: A longitudinal study. *Bilingualism: Language and Cognition, 22*(5), 1160–1175.

DeLuca, V., Rothman, J., Bialystok, E., & Pliatsikas, C. (2019). Redefining bilingualism as a spectrum of experiences that differentially affects brain structure and function. *Proceedings of the National Academy of Sciences, 116*(15), 7565–7574.

DeLuca, V., Rothman, J., Bialystok, E., & Pliatsikas, C. (2020). Duration and extent of bilingual experience modulate neurocognitive outcomes. *NeuroImage, 204*, Article 116222.

Desikan, R. S., Ségonne, F., Fischl, B., Quinn, B. T., Dickerson, B. C., Blacker, D., … Albert, M. S. (2006). An automated labeling system for subdividing the human cerebral cortex on MRI scans into gyral based regions of interest. *Neuroimage, 31*(3), 968–980.

Dhollander, T., Mito, R., Raffelt, D., & Connelly, A. (2019). Improved white matter response function estimation for 3-tissue constrained spherical deconvolution. *Proceedings of the International Society for Magnetic Resonance in Medicine, 555*.

Dhollander, T., Raffelt, D. & Connelly, A. (2016) Unsupervised 3-tissue response function estimation from single-shell or multi-shell diffusion MR data without a co-registered T1 image. ISMRM Workshop on Breaking the Barriers of Diffusion MRI, 5.

Elmer, S., Hänggi, J., Meyer, M., & Jäncke, L. (2011). Differential language expertise related to white matter architecture in regions subserving sensory-motor coupling, articulation, and interhemispheric transfer. *Human Brain Mapping, 32*(12), 2064–2074.

Farquharson, S., Tournier, J. D., Calamante, F., Fabinyi, G., Schneider-Kolsky, M., Jackson, G. D., & Connelly, A. (2013). White matter fiber tractography: Why we need to move beyond DTI. *Journal of Neurosurgery, 118*(6), 1367–1377.

Fischl, B. (2012). FreeSurfer. *Neuroimage, 62*(2), 774–781.

Fornito, A., Zalesky, A., & Bullmore, E. (2016). *Fundamentals of brain network analysis*. Academic Press.

Freeman, L. C. (1978). Centrality in social networks conceptual clarification. *Social Networks, 1*(3), 215–239.

Friederici, A. D. (2009). Pathways to language: Fiber tracts in the human brain. *Trends in Cognitive Sciences, 13*(4), 175–181.

García-Pentón, L., Fernández, A. P., Iturria-Medina, Y., Gillon-Dowens, M., & Carreiras, M. (2014). Anatomical connectivity changes in the bilingual brain. *Neuroimage, 84*, 495–504.

Gold, B. T., Johnson, N. F., & Powell, D. K. (2013). Lifelong bilingualism contributes to cognitive reserve against white matter integrity declines in aging. *Neuropsychologia, 51*(13), 2841–2846.

Gold, B. T., Powell, D. K., Xuan, L., Jiang, Y., & Hardy, P. A. (2007). Speed of lexical decision correlates with diffusion anisotropy in left parietal and frontal white matter: Evidence from diffusion tensor imaging. *Neuropsychologia, 45*(11), 2439–2446.

Gow, D. W., Jr (2012). The cortical organization of lexical knowledge: A dual lexicon model of spoken language processing. *Brain and Language, 121*(3), 273–288.

Green, D. (1998). Mental control of the bilingual lexico-semantic system. *Bilingualism: Language and Cognition, 1*, 67–81.

Green, D. W., & Abutalebi, J. (2013). Language control in bilinguals: The adaptive control hypothesis. *Journal of Cognitive Psychology, 25*(5), 515–530.

Haagort, P. (2005). On Broca, brain, and binding: a new framework. *Trends in Cognitive Sciences, 9*(9), 416–423. https://doi.org/10.1016/j.tics.2005.07.004.

Hagmann, P., Cammoun, L., Gigandet, X., Meuli, R., Honey, C. J., Wedeen, V. J., & Sporns, O. (2008). Mapping the structural core of human cerebral cortex. *PLoS Biology, 6*(7), Article e159.

Hämäläinen, S., Sairanen, V., Leminen, A., & Lehtonen, M. (2017). Bilingualism modulates the white matter structure of language-related pathways. *Neuroimage, 152*, 249–257.

Hermans, D., Bongaerts, T., de Bot, K., & Schreuder, R. (1998). Producing words in a foreign language: Can speakers prevent interference from their first language? *Bilingualism: Language and Cognition, 1*(3), 213–229.

Hickok, G., & Poeppel, D. (2000). Towards a functional neuroanatomy of speech perception. *Trends in Cognitive Sciences, 4*(4), 131–138.

Hickok, G., & Poeppel, D. (2004). Dorsal and ventral streams: A framework for understanding aspects of the functional anatomy of language. *Cognition, 92*(1–2), 67–99.

Hickok, G., & Poeppel, D. (2016). Neural basis of speech perception. *Neurobiology of Language*, 299–310.

Hoenig, K., & Scheef, L. (2005). Mediotemporal contributions to semantic processing: fMRI evidence from ambiguity processing during semantic context verification. *Hippocampus, 15*(5), 597–609.

Hoshino, N., & Thierry, G. (2011). Language selection in bilingual word production: Electrophysiological evidence for cross-language competition. *Brain Research, 1371*, 100–109.

Hosoda, C., Tanaka, K., Nariai, T., Honda, M., & Hanakawa, T. (2013). Dynamic neural network reorganization associated with second language vocabulary acquisition: A multimodal imaging study. *Journal of Neuroscience, 33*(34), 13663–13672.

Jeurissen, B., Leemans, A., Tournier, J. D., Jones, D. K., & Sijbers, J. (2013). Investigating the prevalence of complex fiber configurations in white matter tissue with diffusion magnetic resonance imaging. *Human Brain Mapping, 34*(11), 2747–2766.

Jeurissen, B., Tournier, J. D., Dhollander, T., Connelly, A., & Sijbers, J. (2014). Multi-tissue constrained spherical deconvolution for improved analysis of multi-shell diffusion MRI data. *NeuroImage, 103*, 411–426.

Jones, D. K., Knösche, T. R., & Turner, R. (2013). White matter integrity, fiber count, and other fallacies: The do's and don'ts of diffusion MRI. *NeuroImage, 73*(C), 239–254.

Kellner, E., Dhital, B., Kiselev, V. G., & Reisert, M. (2016). Gibbs-ringing artifact removal based on local subvoxel-shifts. *Magnetic Resonance in Medicine, 76*(5), 1574–1581.

Kousaie, S., Chai, X. J., Sander, K. M., & Klein, D. (2017). Simultaneous learning of two languages from birth positively impacts intrinsic functional connectivity and cognitive control. *Brain and Cognition, 117*, 49–56. https://doi.org/10.1016/j.bandc.2017.06.003.

Kroll, J. F., Sumutka, B. M., & Schwartz, A. I. (2005). A cognitive view of the bilingual lexicon: Reading and speaking words in two languages. *International Journal of Bilingualism, 9*(1), 27–48.

Kroll, J., Bobb, S., Misra, M., & Guo, T. (2008). Language selection in bilingual speech: Evidence for inhibitory processes. *Acta Psychologica, 128*, 416–430.

Kuhl, P. K., Stevenson, J., Corrigan, N. M., van den Bosch, J. J., Can, D. D., & Richards, T. (2016). Neuroimaging of the bilingual brain: Structural brain correlates of listening and speaking in a second language. *Brain and Language, 162*, 1–9.

Latora, V., & Marchiori, M. (2001). Efficient behavior of small-world networks. *Physical Review Letters, 87*(19), Article 198701.

Lee, H., Devlin, J. T., Shakeshaft, C., Stewart, L. H., Brennan, A., Glensman, J., … Price, C. J. (2007). Anatomical Traces of Vocabulary Acquisition in the Adolescent Brain. *Journal of Neuroscience, 27*(5), 1184–1189. https://doi.org/10.1523/JNEUROSCI.4442-06.2007.

Leischner, A. (1987). *Aphasien und Sprachentwicklungsstoerungen*. Stuttgart, Germany: Thieme Verlag.

Leivada, E., Westergaard, M., Duñabeitia, J. A., & Rothman, J. (2021). On the phantom-like appearance of bilingualism effects on neurocognition:(How) should we proceed? *Bilingualism: Language and Cognition, 24*(1), 197–210.

Li, P., & Grant, A. (2016). Second language learning success revealed by brain networks. *Bilingualism: Language and Cognition, 19*(4), 657–664.

Li, P., Legault, J., & Litcofsky, K. A. (2014). Neuroplasticity as a function of second language learning: anatomical changes in the human brain. *Cortex, 58*, 301–324.

Li, L., Abutalebi, J., Emmorey, K., Gong, G., Yan, X., Feng, X., … Ding, G. (2017). How bilingualism protects the brain from aging: Insights from bimodal bilinguals. *Human Brain Mapping, 38*(8), 4109–4124.

Luk, G., Bialystok, E., Craik, F. I., & Grady, C. L. (2011). Lifelong bilingualism maintains white matter integrity in older adults. *Journal of Neuroscience, 31*(46), 16808–16813.

Luk, G., Green, D. W., Abutalebi, J., & Grady, C. (2012). Cognitive control for language switching in bilinguals: A quantitative meta-analysis of functional neuroimaging studies. *Language and Cognitive Processes, 27*(10), 1479–1488.

Mamiya, P. C., Richards, T. L., & Kuhl, P. K. (2018). Right forceps minor and anterior thalamic radiation predict executive function skills in young bilingual adults. *Frontiers in Psychology, 9*, 118.

Marian, V., & Spivey, M. (2003). Competing activation in bilingual language processing: Within-and between-language competition. *Bilingualism: Language and Cognition, 6*(2), 97.

Mechelli, A., Crinion, J. T., Noppeney, U., O'Doherty, J., Ashburner, J., Frackowiak, R. S., & Price, C. J. (2004). Structural plasticity in the bilingual brain. *Nature, 431*(7010), 757.

Nelson, H. E. (1982). *National Adult Reading Test (NART): For the assessment of premorbid intelligence in patients with dementia: Test manual*. Windsor: Nfer-Nelson.

Nichols, E. S., & Joanisse, M. F. (2016). Functional activity and white matter microstructure reveal the independent effects of age of acquisition and proficiency on second-language learning. *Neuroimage, 143*, 15–25.

Oh, A., Duerden, E. G., & Pang, E. W. (2014). The role of the insula in speech and language processing. *Brain and Language, 135*, 96–103.

Oldfield, R. C. (1971). Edinburgh handedness inventory. *Neuropsychologia, 9*, 97–113.

Owen, J. P., Li, Y. O., Ziv, E., Strominger, Z., Gold, J., Bukhpun, P., … Mukherjee, P. (2013). The structural connectome of the human brain in agenesis of the corpus callosum. *Neuroimage, 70*, 340–355.

Parker Jones, Ō., Green, D. W., Grogan, A., Pliatsikas, C., Filippopolitis, K., Ali, N., … Seghier, M. L. (2012). Where, when and why brain activation differs for bilinguals and monolinguals during picture naming and reading aloud. *Cerebral Cortex, 22*(4), 892–902.

Pernet, C. R., Wilcox, R. R., & Rousselet, G. A. (2013). Robust correlation analyses: False positive and power validation using a new open source matlab toolbox. *Frontiers in Psychology, 3*, 606.

Pliatsikas, C. (2019). Multilingualism and brain plasticity. In J. W. Schwieter (Ed.), *The handbook of the neuroscience of multilingualism* (pp. 230–251). Wiley Blackwell.

Pliatsikas, C. (2020). Understanding structural plasticity in the bilingual brain: The Dynamic Restructuring Model. *Bilingualism: Language and Cognition, 23*(2), 459–471.

Pliatsikas, C., Moschopoulou, E., & Saddy, J. D. (2015). The effects of bilingualism on the white matter structure of the brain. *Proceedings of the National Academy of Sciences, 112*(5), 1334–1337.

Pötzl, O. (1925). Ueber die parietal bedingte Aphasie und ihren Einfluss auf das Sprechen mehrerer Sprachen. *Zeitschrift für die gesamte Neurologie und Psychiatrie, 96*(1), 100–124.

Rahmani, F., Sobhani, S., & Aarabi, M. H. (2017). Sequential language learning and language immersion in bilingualism: Diffusion MRI connectometry reveals microstructural evidence. *Experimental Brain Research, 235*(10), 2935–2945.

Reverberi, C., Kuhlen, A., Abutalebi, J., Greulich, R. S., Costa, A., Seyed-Allaei, S., & Haynes, J. D. (2015). Language control in bilinguals: Intention to speak vs. execution of speech. *Brain and Language, 144*, 1–9.

Rodriguez-Fornells, A., Kramer, U., Lorenzo-Seva, U., Festman, J., & Münte, T. F. (2012). Self-assessment of individual differences in language switching. *Frontiers in Psychology, 2*, 388.

Rubinov, M., & Sporns, O. (2010). Complex network measures of brain connectivity: Uses and interpretations. *Neuroimage, 52*(3), 1059–1069.

Sampaio-Baptista, C., & Johansen-Berg, H. (2017). White matter plasticity in the adult brain. *Neuron, 96*(6), 1239–1251.

Saur, D., Kreher, B. W., Schnell, S., Kümmerer, D., Kellmeyer, P., Vry, M. S., … Weiller, C. (2008). Ventral and dorsal pathways for language. *Proceedings of the National Academy of Sciences, 105*(46), 18035–18040.

Singh, N. C., Rajan, A., Malagi, A., Ramanujan, K., Canini, M., Della Rosa, P. A., … Abutalebi, J. (2018). Microstructural anatomical differences between bilinguals and monolinguals. *Bilingualism: Language and Cognition, 21*(5), 995–1008.

Smith, R. E., Tournier, J. D., Calamante, F., & Connelly, A. (2012). Anatomically-constrained tractography: Improved diffusion MRI streamlines tractography through effective use of anatomical information. *Neuroimage, 62*(3), 1924–1938.

Smith, R. E., Tournier, J. D., Calamante, F., & Connelly, A. (2015). SIFT2: Enabling dense quantitative assessment of brain white matter connectivity using streamlines tractography. *Neuroimage, 119*, 338–351.

Smith, S. M., Jenkinson, M., Woolrich, M. W., Beckmann, C. F., Behrens, T. E., Johansen-Berg, H., … Niazy, R. K. (2004). Advances in functional and structural MR image analysis and implementation as FSL. *Neuroimage, 23*, S208–S219.

Stein, M., Federspiel, A., Koenig, T., Wirth, M., Strik, W., Wiest, R., … Dierks, T. (2012). Structural plasticity in the language system related to increased second language proficiency. *Cortex, 48*(4), 458–465.

Sulpizio, S., Toti, M., Del Maschio, N., Costa, A., Fedeli, D., Job, R., & Abutalebi, J. (2019). Are you really cursing? Neural processing of taboo words in native and foreign language. *Brain and language, 194*, 84–92.

Sulpizio, S., Del Maschio, N., Del Mauro, G., Fedeli, D., & Abutalebi, J. (2020). Bilingualism as a gradient measure modulates functional connectivity of language and control networks. *NeuroImage, 205*, Article 116306.

Sulpizio, S., Del Maschio, N., Fedeli, D., & Abutalebi, J. (2020). Bilingual language processing: A meta-analysis of functional neuroimaging studies. *Neuroscience & Biobehavioral Reviews, 108*, 834–853.

Surrain, S., & Luk, G. (2017). Describing bilinguals: A systematic review of labels and descriptions used in the literature between 2005–2015. *Bilingualism: Language and Cognition*, 1–15.

Taylor, R. (1990). Interpretation of the correlation coefficient: A basic review. *Journal of Diagnostic Medical Sonography, 6*(1), 35–39.

Tournier, J. D., Calamante, F., & Connelly, A. (2010). Improved probabilistic streamlines tractography by 2nd order integration over fibre orientation distributions. In Proceedings of the international society for magnetic resonance in medicine (Vol. 1670). Ismrm.

Tournier, J. D., Smith, R., Raffelt, D., Tabbara, R., Dhollander, T., Pietsch, M., … Connelly, A. (2019). MRtrix3: A fast, flexible and open software framework for medical image processing and visualisation. *NeuroImage, 202*, Article 116137.

Van Heuven, W. J., Mandera, P., Keuleers, E., & Brysbaert, M. (2014). SUBTLEX-UK: A new and improved word frequency database for British English. *Quarterly Journal of Experimental Psychology, 67*(6), 1176–1190.

Veraart, J., Novikov, D. S., Christiaens, D., Ades-Aron, B., Sijbers, J., & Fieremans, E. (2016). Denoising of diffusion MRI using random matrix theory. *Neuroimage, 142*, 394–406.

Virtanen, P., Gommers, R., Oliphant, T. E., Haberland, M., Reddy, T., Cournapeau, D., … van der Walt, S. J. (2020). SciPy 1.0: Fundamental algorithms for scientific computing in Python. *Nature Methods, 17*(3), 261–272.

Zalesky, A., Fornito, A., & Bullmore, E. T. (2010). Network-based statistic: Identifying differences in brain networks. *Neuroimage, 53*(4), 1197–1207.